EVALUATION OF OSIRIX SOFTWARE WITH CRANIOFACIAL ANTHROPOMETRIC PURPOSES

DIAS, Paulo Eduardo Miamoto*
BEAINI, Thiago Leite**
MELANI, Rodolfo Francisco Haltenhoff***

ABSTRACT

Forensic Facial Reconstruction is a branch of Forensic Anthropology that attempts to approximate the appearance of an unknown individual through soft tissue reconstruction, after anthropological craniofacial analysis is carried out. The reconstruction publicized in the media aims at a recognition, which can trigger formal human identification. Knowing the anthropometric relationships between hard and soft tissues is useful to increase the accuracy of reconstructions. It was sought to evaluate the performance of the software OsiriX as a tool for anthropometric analysis of both hard and soft tissues. In cone beam CBCT scans of eight individuals, seven linear distances, determined by 14 anatomical landmarks on hard and soft tissues were measured. Intra-observer and inter-observer variation were evaluated by two criteria: reproducibility of landmark location on skull surface and reproducibility of measurement values in millimeters. For intra-observer evaluation, the sample was measured twice within an interval of two weeks. To assess inter-observer variation three independent operators performed measurements once. For reproducibility of anatomical landmarks, the metadata containing the distance in millimeters from each point to the origin of the x, y and z axis were obtained from the software. Means and standard deviations for the set of linear measurements and coordinates of the points were analyzed, and the difference between the standard deviations was used to classify reproducibility. For intra and inter-observer variations, most of the landmarks were located with less than 0.5mm of difference between measurements. For the corresponding measurements, made between these landmarks, most were repeated with less than 1.5 mm of difference for both intra and inter-observer variation. In practical terms, the differences detected did not hamper the use of the software as a tool for anthropometric studies. The use of OsiriX is an alternative for anthropological study of craniofacial hard and soft tissues from CBCT.

KEYWORDS

Forensic Anthropology. Forensic Dentistry. Anthropometry. Cone-beam computed tomography. Forensic Facial Reconstruction.

PhD, CAPES Foundation, Ministry of Education of Brazil, Brasília, DF, Brazil*
PhD, Laboratory of Forensic Anthropology and Dentistry, Faculty of Dentistry, University of São Paulo, SP, Brazil **
PhD, Professor and Head of the Laboratory of Forensic Anthropology and Dentistry, Faculty of Dentistry, University of São Paulo, SP, Brazil***
Correspondence: dr.miamoto@gmail.com (DIAS PEM) | **Received** 10 Nov 2013 **Received in revised form** 11 Nov 2013 **Accepted** 13 Nov 2013

INTRODUCTION

Forensic facial reconstruction (FFR) techniques are an attempt to recreate the approximate facial features of an individual, after an anthropological analysis and modeling direct on to a skull or its cast. That may also be obtained virtually using software, in order to increase the chances of recognition and a possible human identification.[1] This technique can also be performed apart from forensic context, for archaeological, historical, artistic, museological and educational purposes.[2] It can be performed in three dimensions (3D) using plastic material, such as clay, or made in virtual computerized environment. It can also be accomplished in two dimensions (2D), by manual or computer-assisted drawings over photographs of a skull.

The cranial bones form the framework on which craniofacial soft tissues insert themselves. Despite a general basic structure similar to the human species, variations related to gender, age, nutritional status, ancestry and the presence of diseases can significantly alter the dynamics of the interaction between bones and muscular, adipose and glandular soft tissues.[2,3] The result is an increase in the degree of individuality of the human face, which makes each one unique and distinguishable.[2]

Studies on how soft tissues develop, grow age and react to external factors can assist in the reconstruction of facial characteristics of an individual. There are researches that approach soft tissues of the face in its totality[4] or on specific areas such as the ears,[5] orbits,[6] orofacial region,[7] nose,[8] among others.

In order to reconstruct facial anatomy, soft tissue depth data is recommended. Therefore research also deals with the collection of anthropological data on average soft tissue depths, according to the origin of each group studied.[1,9-17]

A third area of advances in FFR concerns the development of automated and computerized techniques for reconstruction.[18] Technological progress enables the application of new tools with forensic purposes, like medical imaging devices or surface scanners, that can be portable or bench top.[19-22] The use of these tools allows advances on all search fields cited above. A virtual 3D model can be obtained from DICOM images (digital imaging and communications in Medicine), which can be generated from various medical exams, such as cone-beam computed tomography (CBCT). Transforming a face into a 3D virtual model has promising implications for Forensic Anthropology since its digital storage allows one to perform research, on the cited areas creating digital anthropological databases, where access to an entire collection could be granted to remote researchers of several fields and expertise, without the risk of damaging the material. If necessary, the 3D models can be

"printed" by prototyping, and turned into physical replicas of the original skulls. However, an important limitation of 3D models is that they fail to provide any other kind of feedback besides the visual one.

In this context, the aim of this study was to analyze the performance of a software application as a tool for anthropometric studies. It was aimed to verify whether it might be used for research in FFR, specifically for assessing the interaction between hard and soft facial tissues of an individual.

MATERIAL AND METHODS

This research was submitted to analysis and approved by the local Research Ethics Committee of the Faculty of Dentistry, under protocol number 129/11.

Computer folders containing digital imaging and communications in Medicine (DICOM) files originated from cone-beam computerized tomography (CBCT) scans of eight adult women with ages between 25 and 59 years (mean age 44 years), identified only by numeric codes. DICOM files were obtained with an iCat imaging device (Hatfield, PA, USA). There was no information about ancestry, medical/dental history or nutritional status of the surveyed individuals. The thickness of slices that originated DICOM images was 0.20 mm.

The data were imported in open-access biomedical DICOM viewer software OsiriX (version 5.0.2 32-bit) (Bernex, Switzerland), installed on a MacBook Pro notebook (Cupertino, USA) (Intel Core i5 2.3 GHz, graphic card Intel HD Graphics 3000 384 MB and 6 GB RAM) with Mac OS X 10.7.5 operational system.

The scans had mandible and maxilla in occlusion, with upper and lower lips in contact, in neutral facial expression. All DICOMs showed entirely the facial and craniometric landmarks[3,17,23,24] in table 1.

Landmark location:

Three-dimensional volume rendering view was generated, in which a 3D virtual object is rendered from two-dimensional (2D) images of the three axis (sagittal, axial and coronal) acquired in the CBCT exam. This view allows the operator to zoom in and rotate freely the rendered volume. “Bone” view mode was selected, showing rendered surfaces with radiodensities compatible with bony tissue. Thus, it was possible to locate points and pin red spheres on craniometric landmarks of the sample (table 1) by using the "point" tool.

Afterwards, view mode was changed to “skin” setting and the four anthropometric soft tissue landmarks of the mouth[3] were marked according to guidelines[24] of 3D rendered volumes (Fig. 1).

All landmarks, designated by the software as Regions of Interest (ROI) were exported into spreadsheets with their spatial coordinates, measured in millimeters, indicating their distance from the origin of each axis (x, y, z) within the field of view of the CT scanner. The axis x, y and z, thus refer to the distances in lateral-lateral, ventral-dorsal and cranial-caudal directions, respectively. For both intra-observer and inter-observer variations, differences between sets of

measurements of each axis were verified by analysis of variance (ANOVA) tests (CI 95%, p=0.05).

The mean and standard deviations for each axis, that represented the whole set of coordinates, were calculated for each landmark. Reproducibility was assessed by the difference between the standard deviations of each observation.

The reproducibility of the anatomical landmarks was evaluated as:[25] great, when the value of the difference between standard deviations was less than 0.5 mm, good when it fell between 0.5 mm and 1 mm and regular, if it was above 1 mm. Thus, it was possible to analyze if during the process of landmark location, the largest variations of each landmark happened towards lateral-lateral (x axis), ventral-dorsal (y axis) or cranial-caudal (z axis) direction. By doing this, it was sought to evaluate if linear measurements were starting from similar locations on the skull.

The maximum distances between the landmarks located on the CBCT for each set of measurements were calculated using the means of each axis. The differences between the average values of the coordinates, for each axis, were used to calculate the distance between the landmarks located by the observers. By subtracting the averages of the observations among each other, for both intra-observer and inter-observer variations, the maximum and minimal distances between located landmarks were calculated. Using the largest differences between the averages, the maximum distance between the locations of a same landmark was calculated from ROI coordinates (e.g.: for chr, on intra-observer variation) with the formula:

$$dmax = \sqrt{(x1 - x2)^2 + (y1 - y2)^2 + (z1 - z2)^2}$$

The symbols inside the brackets represent the largest difference calculated between the ROI coordinates for each axis.

Using the smallest differences between the averages for each axis, the same formula was applied for calculating the minimum distance between the locations of a same landmark:

$$dmin = \sqrt{(x1 - x2)^2 + (y1 - y2)^2 + (z1 - z2)^2}$$

The symbols inside brackets represent the smallest differences calculated from the averaged ROI coordinates. Thus, the effects caused by variations on the three axis could be evaluated as a whole, in mm.

Linear distance measurement:

Three-dimensional multiplanar rendering view was activated (3D MPR), which renders a 3D object with its view in two dimensions, divided into simultaneously displayed anatomical planes (sagittal, transverse and coronal).

The advantage of the 3D MPR mode is that the operator can locate a landmark on a slice that can be viewed simultaneously in the other planes' windows. The projected reference lines identify the perpendicular relation of both planes shown simultaneously on the other windows. When a reference line is rotated, the perpendicular alignment between the two plans is maintained. Therefore, it is possible to cross planes in a controlled manner to identify two of the landmarks

previously marked in the 3D volume rendering view mode in one single slice (Fig. 2).

To perform the linear measurements using the "length" tool, the thickness of the viewed slices was increased to 2.5 mm with Maximum Intensity Projection (MIP) view and zoom was adjusted to 160% in the window of the coronal plane (chosen by convenience), in which linear measurements were made. Thus, the alignment of anatomical landmarks in the three planes was facilitated, since the increased thicknesses were automatically applied to all planes, favoring correct alignment. To ensure that linear measurements were properly made, in the window of the sagittal plane, the line corresponding to the coronal plane (vertical on the sagittal plane window (upper left on the screen) and horizontal on the axial plane window (lower left)) was corrected to cross two of the landmarks whose distance were to be measured. Then, in the window of the coronal plane, the same process was repeated to sagittal plane guide line (vertical on both axial (lower left) and coronal (right) windows). Thus, the landmarks located along the sagittal line were adequately aligned and their measurements could also be properly taken in the coronal plane window, as it was expected that same value would be obtained in both views (Fig. 3). For bilateral points, the same process was used in the window of the transverse plane, with the measurements made in the coronal plane window.

Measurements were taken between the landmarks: PM-SD, ID-SM, ls-li, NS-GN, MLr-MLl, CNr-CNl and chr-chl.

For the assessment of intra-observer variation, one of the authors of this study (operator 1) took measurements three times, with an interval of 2 weeks between them. The evaluation of the inter-observer variation was performed similarly to the intra-observer variation, with operator 1 and two other control operators (operators 2 and 3) performing landmark location and linear measurements. Previously to measurements, control operators 2 and 3 underwent a calibration period where they were instructed on the use of OsiriX, the location of landmarks and measurement procedures. Once calibrated, operator 1 assisted the control operators on the use of commands and features of the software in case of doubt, but did not interfere on the location of anatomical landmarks on the images that appeared on the screen.

For each of the linear measurements, means and standard deviations for each operator were calculated. Reproducibility was assessed by the difference between the standard deviations.

In the 3D MPR window, the anatomical landmark displayed is shown as a point of same size regardless of zoom setting. It is represented by a green double circle, with default value of about 6 pixels, or 1.5 mm diameter. To use the "length" tool the operator must manually draw a line between the two points at the center of the green circles. Thus, the values of the measurements could assume values within expected deviations of ± 1.5 mm in their actual length. The reproducibility of the set of measurements was considered: great when the difference between their standard deviations did not exceed 1.5 mm, good when it was between 1.5 mm and 3 mm and regular when exceeded this value.

The difference between the highest and lowest standard deviations among the three operators was taken into account to classify the reproducibility of landmark location and linear

measurements. The criteria for classification of the reproducibility of landmark location and linear measurements were the same for intra and inter-observer variations.

Figure 1 - 3D MPR view, showing landmarks located on hard (left) and soft tissues (right).

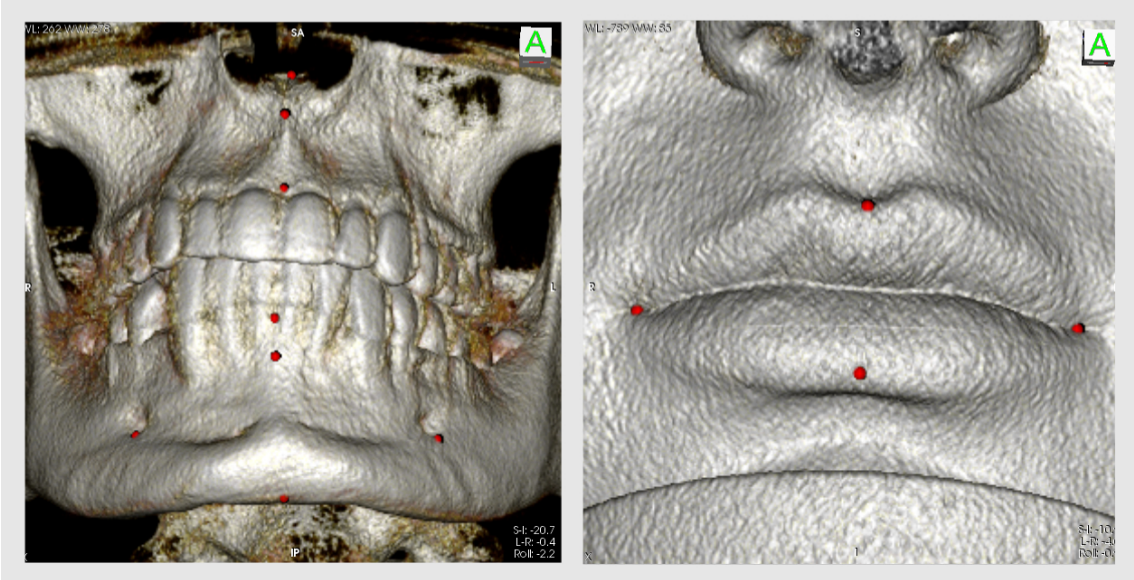

Figure 2 - alignment of landmarks PM and SD using reference lines on window of sagittal (upper left) and coronal (right) planes.

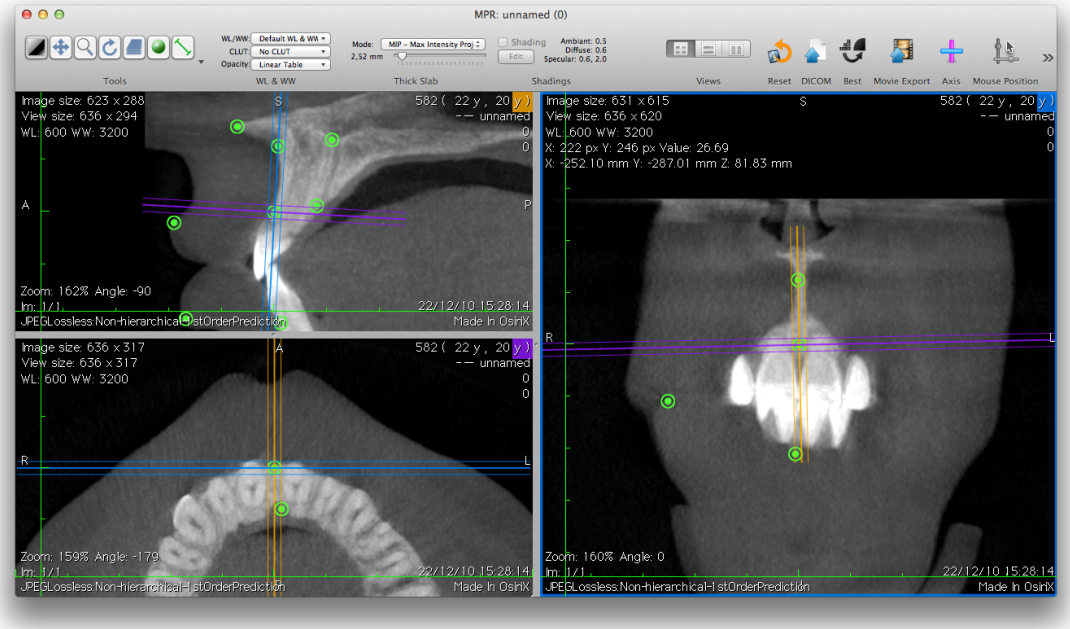

Figure 3 - linear measurements made with the "length" tool, showing that measurements made on the coronal plane, based on the alignment of the sagittal plane, have the same value, independently from the plane view.

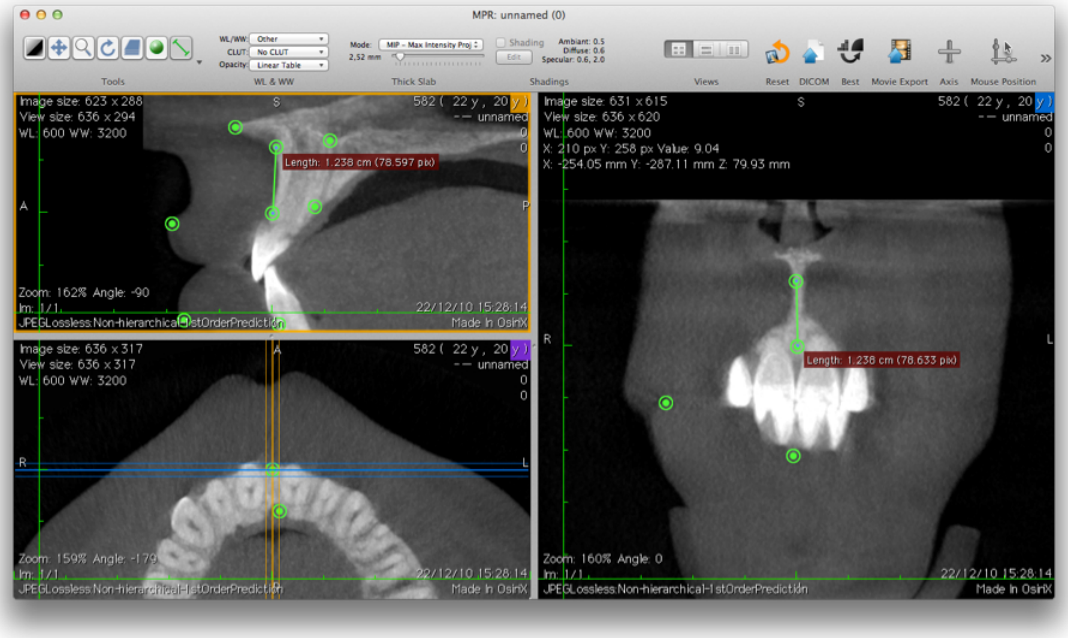

RESULTS

Landmark location:

The coordinate values for the three axis, for intra-observer and inter-observer landmark location are shown in tables 2 and 3, respectively. None of the sets of measurements for each axis, for both intra-observer and inter-observer variations had statistically significant differences amongst them, according to the results of ANOVA tests ($p>0.05$, CI 95%). The maximum and minimum distances between the locations of each landmark, for intra-observer and inter-observer variations, are shown on table 4.

Table 1 – Anatomic landmarks on hard (abbreviated in upper case) and soft tissues (abbreviated in lower case) used for linear measurements.

	Landmark	Abbreviation	Description
	Median		
1	*Nasospinale*	NS	Lowest point of the lower ridge of the piriform opening, on the base of the nasal spine, projected on the sagittal plane
2	*Philtrum medium*	PM	On the maxilla, bellow the curvature of the nasal spine
3	*Supradentale*	SD	Most anterior and superior point of the alveolar ridge, between the central upper incisors
4	*Infradentale*	ID	Most anterior and superior point of the alveolar ridge, between the central lower incisors
5	*Supramentale*	SM	On the midline, located in the depression between the mental eminence and the roots of the central lower incisors

6	*Gnathion*	GN	Point on the anterior portion of the mandible that projects itself lowermost on the sagittal plane
7	*Labiale superius*	ls	Midpoint on the upper lip vermillion
8	*Labiale inferius*	li	Midpoint on the lower lip vermillion
	Bilateral (r - right; l - left)		
9	*Canini*	CNr, CNl	On the buccodistal surface of the upper canines, at the level of the interproximal contact with premolars
10	*Mentale*	MLr, MLl	Lowermost point of the mental foramen
11	*Cheilion*	chr, chl	On the corners of the mouth

Table 2 – Intra-observer reproducibility for landmark (L) location, with the averages for the whole group of CBCTs measured, on first (A Obs1), second (A Obs2) and third (A Obs 3) observations. Reproducibility (Rep) evaluated by the difference (DSD) between standard deviations (SD1, SD 2 and SD3) on the first and second observations. Classified as regular if DSD>1.00 mm, good if 0.5 mm<DSD<1.00 mm and great if 0 mm<DSD<0.5 mm. Continues on next page.

L		A Obs 1	A Obs 2	A Obs 3	SD 1	SD 2	SD 3	DSD	Rep
NS									
	x	301.35	301.79	301.50	27.1	26.49	26.90	0.61	Good
	y	354.1	354.39	353.74	26.88	26.46	25.79	1.09	Regular
	z	85.8	85.98	85.48	7.67	7.44	8.15	0.71	Great
PM									
	x	302.13	302.26	301.99	26.25	26.22	27.05	0.83	Great
	y	351.31	351.52	351.52	25.48	25.57	25.86	0.38	Great
	z	80.64	80.66	79.86	7.3	7.25	6.79	0.51	Good
SD									
	x	302.36	302.41	302.27	26.85	26.86	27.05	0.20	great
	y	355.69	355.8	355.64	26.7	26.08	25.86	0.84	good
	z	71.02	70.83	71.97	6.14	7.08	6.79	0.94	good
CNr									
	x	319.84	320.04	320.12	27.42	27.23	27.21	0.21	great
	y	347.06	347.13	347.05	26.04	26.17	26.12	0.13	great
	z	63.96	64.05	63.27	6.6	6.73	6.42	0.31	great
CNl									
	x	284.16	284.1	283.92	26.41	26.28	26.32	0.13	great
	y	347.52	347.67	347.33	26.16	26.13	26.33	0.20	great
	z	63.96	63.94	63.56	6.3	6.13	5.86	0.44	great
ID									
	x	303.31	303.2	303.10	27.92	28.05	28.17	0.25	great
	y	353.88	353.77	353.90	27.27	27.16	27.22	0.11	great
	z	49.72	49.49	49.69	5.14	5.27	5.61	0.12	great
SM									
	x	303.33	302.99	303.39	27.95	28.96	28.15	1.01	regular

	x	352.17	352.09	352.20	28.53	28.63	28.49	0.14	great
	z	43.98	44.01	44.16	5.39	5.24	6.02	0.78	good
MLr									
	x	324.71	324.72	324.53	27.77	27.69	27.81	0.12	great
	y	338.89	338.77	338.84	27.33	27.28	27.31	0.05	great
	z	35.92	35.99	36.04	5.62	5.61	5.75	0.14	great
MLl									
	x	279.88	279.85	279.98	27.88	27.86	27.90	0.04	great
	y	341.25	341.12	341.06	28.9	28.95	29.13	0.23	great
	z	35.38	35.29	35.49	5.36	5.41	5.29	0.12	great
GN									
	x	302.64	302.98	302.69	27.99	26.97	27.83	1.02	regular
	y	350.24	349.85	349.95	28.77	28.78	28.73	0.05	great
	z	22.31	22.28	22.31	5.8	5.96	5.86	0.16	great
ls									
	x	302.33	302.52	302.49	27.29	27.51	27.65	0.36	great
	y	369.59	369.3	369.51	26.9	27.47	26.89	0.58	good
	z	67.14	67.33	68.49	6.72	6.9	7.38	0.66	great
li									
	x	302.65	302.61	303.05	27.44	27.8	27.50	0.36	great
	y	368.45	368.39	368.55	27.43	27.48	27.57	0.14	great
	z	54.48	54.6	55.04	6.88	6.78	6.49	0.39	great
cbr									
	x	324.24	324.55	325.65	26.77	26.73	26.88	0.15	great
	y	354.26	354.34	352.63	27.96	28.03	28.14	0.18	great
	z	57.83	57.71	56.70	6.1	6.27	5.54	0.73	good
cbl									
	x	280.15	280.32	279.70	28.06	27.94	27.87	0.19	great
	y	355.94	356.1	355.89	28.64	28.9	28.59	0.26	great
	z	57.49	57.38	57.30	6.23	6.22	6.21	0.02	great

Table 3 – Inter-observer reproducibility for landmark location, with the averages for the whole group of CBCTs measured, divided by their average value for the three operators (A Op1, A Op2 and A Op3) and standard deviations for each of them (SD 1, SD 2, SD 3). Reproducibility (Rep) evaluated by the difference between larger and smaller standard deviations between the 3 operators, classified as regular if DSD>1.00 mm, good if 0.5 mm<DSD<1.00 mm and great if 0 mm<DSD<0.5 mm. Continues on next page

L		A Op1	A Op2	A Op3	SD 1	SD 2	SD 3	DSD	Rep
NS									
	x	301.35	302.15	301.98	27.10	26.99	26.51	0.59	good
	y	354.10	352.40	354.62	26.88	26.70	26.35	0.53	good
	z	85.80	85.94	85.96	7.67	7.62	7.47	0.20	great
PM									
	x	302.13	301.88	302.01	26.25	26.37	26.29	0.12	great
	y	351.31	351.77	351.53	25.48	25.68	25.58	0.20	great
	z	80.64	81.44	80.00	7.30	7.62	7.56	0.59	great
SD									
	x	302.36	302.33	302.39	26.85	26.68	26.86	0.18	great
	y	355.69	355.51	355.57	26.70	26.38	26.57	0.32	great
	z	71.02	71.43	71.48	6.14	6.94	6.52	0.81	good
CNr									
	x	319.84	318.43	319.86	27.42	26.91	27.26	0.51	good
	y	347.06	349.68	347.57	26.04	26.67	25.82	0.84	good
	z	63.96	63.44	63.56	6.60	7.10	6.57	0.53	good
CNl									
	x	284.16	283.05	284.09	26.41	26.54	26.37	0.17	great
	y	347.52	349.40	347.61	26.16	26.50	26.06	0.34	great
	z	62.97	63.96	63.66	6.35	6.30	6.76	0.46	great
ID									
	x	303.31	303.06	303.26	27.92	28.09	28.12	0.20	great
	y	353.88	353.44	353.70	27.27	26.71	27.45	0.74	good
	z	49.72	50.04	49.58	5.14	4.86	5.43	0.56	good
SM									
	x	305.33	303.33	303.27	29.34	27.95	28.28	1.39	regular
	y	352.17	352.30	351.86	28.53	28.42	29.18	0.76	good
	z	43.98	43.55	44.39	5.39	5.68	6.23	0.29	great
MLr									
	x	325.09	324.80	324.44	27.95	27.96	28.00	0.01	great
	y	338.89	338.73	339.05	27.33	27.15	27.30	0.18	great
	z	35.92	36.15	36.02	5.62	5.40	5.44	0.22	great
MLl									
	x	279.88	279.84	280.42	27.88	27.92	27.79	0.13	great
	y	341.25	340.44	341.64	28.90	28.96	28.93	0.07	great
	z	35.38	35.32	35.51	5.36	5.24	5.38	0.13	great
GN									
	x	302.64	303.02	302.77	27.99	28.03	27.97	0.04	great
	y	350.24	350.59	349.92	28.77	28.91	28.68	0.23	great
	z	22.31	22.18	22.28	5.80	5.91	5.96	0.16	great
ls									
	x	302.33	302.34	302.78	27.29	27.93	27.47	0.63	good
	y	369.59	366.97	369.25	26.90	26.13	27.05	0.92	good
	z	67.40	67.63	67.40	6.64	6.84	7.35	0.70	good
li									
	x	302.65	302.78	302.84	27.44	27.89	27.71	0.18	great
	y	368.45	368.32	368.27	27.43	27.45	27.45	0.02	great
	z	54.48	54.16	54.08	6.88	6.21	6.90	0.69	good
chr									
	x	323.94	324.50	323.67	27.60	28.15	27.17	0.99	good
	y	354.56	354.19	354.98	27.11	26.67	26.99	0.44	great
	z	57.83	57.66	57.98	6.10	6.57	6.20	0.47	great
chl									
	x	280.15	279.62	280.39	28.06	27.56	27.59	0.50	great
	y	355.94	355.50	356.57	28.64	28.59	28.39	0.25	great
	z	57.49	56.95	57.61	6.23	6.42	6.15	0.27	great

Table 4 – Maximum (dmax), minimum (dmin) and average distances, in mm. between the landmarks (L) located on both intra-observer (three left columns) and inter-observer (three right columns) observations.

	Intra			Inter		
L	dmax	dmin	Average	dmax	dmin	Average
NS	0.93	0.37	0.65	2.23	0.55	1.39
PM	0.87	0.13	0.50	1.53	0.69	1.11
SD	1.17	1.15	1.16	0.50	0.08	0.29
CNr	0.83	0.12	0.48	3.03	0.52	1.78
CNl	0.51	0.16	0.33	2.40	0.32	1.36
ID	0.33	0.10	0.22	0.68	0.23	0.46
SM	0.47	0.07	0.27	2.23	0.43	1.33
MLr	0.25	0.07	0.16	0.76	0.35	0.55
MLl	0.30	0.11	0.21	1.35	0.40	0.87
GN	0.52	0.11	0.32	0.78	0.35	0.56
ls	1.39	1.16	1.28	2.67	0.34	1.50
li	1.45	0.15	0.80	0.48	0.11	0.29
chr	2.49	0.14	1.31	1.19	0.48	0.84
chl	0.68	0.19	0.44	1.47	0.52	0.99

Linear distance measurements:

Results for linear measurements are displayed in two tables for intra-observer variation and in two tables for inter-observer variation. Tables 5 and 7 show values, in mm, for linear distances of each individual examined, for intra-observer and inter-observer evaluation, respectively. Tables 6 and 8 show average values for the whole set of measurements and evaluates linear distance reproducibility based on average values and difference standard deviations.

DISCUSSION

One of the most important aspects for validation of this methodology, besides the actual evaluation of measurement values, was the verification of the anatomical landmarks that originated them. Given the importance of adequately knowing their location,[3] be it on a living individual or a cadaver, for measurements taken in situ or in a virtual environment, it was observed that more than similarity of values in mm, operators were able to locate landmarks with less than 1 mm of discrepancy, in general.

Some authors[25] detected intra-observer and inter-observer concordance of less than 0.2 mm between points chr, chl, ls and li. Although our results do not indicate the same accuracy

in reproducibility, nor less inaccurate results than those of previous publications,[26] landmarks in soft tissues showed values within a range considered great or good. It is important to highlight that working with soft tissue anatomical landmarks from CBCT scans is difficult, because even though there are guidelines for the examination and location of these landmarks on 3D models,[24] volumes rendered from CBCT scans were not created for soft tissue analysis purposes, and are more suitable for working with hard tissue structures. Moreover, unlike the manual exam, one cannot ask the individual to facilitate the location of landmarks in soft tissue, like by asking the subject to open the mouth to locate the cheillion points. Additionally, artifacts inherent to the CBCT technique, originated from metallic objects inside the mouth, can hamper the location of anatomical structures in regions affected by these artifacts, such as the cheillions and labial points. This was reflected in some of soft tissue landmarks displaying differences between locations on the axis close to 1 mm (ls and chr), which still did not make them irreproducible.

In 3D scans, for example, this phenomenon is not present, since the surface of the face is captured, with the possibility of color texturizing, which adds features that facilitate the location of landmarks of the mouth, favoring the location of the transition zone between skin and lip vermillion. In CBCTs, this is a difficult task, requiring attention to differences of surface textures, that tend to be subtle and without color differentiation (especially when identifying the transition zone between skin and mouth vermillion). This may contribute to lower the reproducibility of landmark placement and the corresponding linear measurements. However, working with CBCT has a significant feature that makes these difficulties acceptable: it is possible to evaluate the direct relations between soft and hard tissues.

The locations of ID and SD landmarks can be difficult depending on the bony level of the alveolar portion. However, in intra- and inter-observer variations, despite the largest discrepancies were detected in y and z axis (dorsal-ventral and cranial-caudal directions), these were considered within an acceptable standard of reproducibility. The observed discrepancies may be characterized as being higher towards cranial-caudal direction (z axis), since sometimes the limits of the alveolar crest can be difficult to visualize. Following these variations of the z axis, the ones of y axis (dorsal-ventral) indicate that with the variation on the height of the points ID and SD, the convexity of the buccal surface of the alveolar process also varies, causing these differences. At the PM, where a greater variation would be expected due to difficulty in locating a concavity below the nasal spine in a virtual environment, there was great

reproducibility in all three axis. Landmark SM showed only a good reproducibility towards lateral-lateral directions and very good reproducibility towards cranial-caudal direction. Thus, the variations in location were associated to the distance of the landmark from the midline towards the left or right sides, whilst they were at the same height of the alveolar process of the mandible, therefore indicating that the concavity that defines it had been properly located.

Table 5 – Values for linear distances, in mm, for first and second measurements (Obs 1, Obs 2 and Obs 3), for each subject, for evaluation of intra-observer variation.

Indivíduo	PM-SD	ID-SM	ls-li	NS-GN	MLr-MLl	CNr-CNl	chr-chl
Obs 1							
1118	12.74	5.46	11.79	68.14	45.76	37.17	37.22
1264	12.63	6.56	17.29	69.79	43.46	34.70	44.95
1265	8.57	5.38	10.31	62.52	42.09	38.69	42.14
1271	9.07	4.88	10.10	60.86	46.67	34.55	42.51
1272	9.14	5.61	13.10	53.27	48.20	37.26	47.72
1281	13.68	6.15	20.2	69.32	45.48	39.30	45.71
1283	8.92	5.85	7.63	64.14	43.94	34.15	44.34
1284	9.86	8.34	14.72	63.83	44.94	33.19	47.41
Obs 2							
1118	7.73	6.01	11.29	69.23	46.69	37.54	40.76
1264	12.74	5.82	17.59	63.07	43.21	32.69	42.83
1265	8.84	5.68	10.19	63.18	42.72	37.48	42.26
1271	9.10	4.73	9.72	61.02	46.34	34.33	45.02
1272	8.54	4.55	13.79	43.24	47.67	37.00	46.23
1281	13.48	6.64	18.85	68.87	44.70	39.08	44.77
1283	8.67	6.40	9.00	63.88	43.23	33.94	41.85
1284	14.66	8.65	13.11	64.99	45.71	33.00	47.43
Obs 3							
1118	9.97	5.52	11.13	68.54	44.83	37.66	38.67
1264	11.83	5.89	16.7	69.43	42.77	35.42	45.7
1265	8.02	5.78	11.67	62.59	42	38.52	43.8
1271	8.77	4.6	10.65	60.75	47.03	34.87	45.83
1272	8.31	4.04	13.66	53.02	48.08	37.17	48.26
1281	13.79	6.72	18.57	69.73	45.42	38.71	47.68
1283	8.21	6.48	8.69	64.14	42.11	34.18	45.07
1284	11.85	8.59	13.33	64.29	45.1	34.24	48.59

Table 6 – Averages of linear distances in mm, for intra-observer variation after first (Obs 1) and second (Obs 2) measurements. Difference between (DSD) standard deviations (SD 1 and SD 2) were used to evaluate measurement reproducibility, considered good when 1.5 mm<DSD<3.0 mm or great when 0 mm<DSD<1.5 mm.

Measure	Obs 1	Obs 2	SD 1	SD 2	DSD	Reproducibility
PM-SD	10.58	10.47	2.08	2.69	0.62	great
ID-SM	6.03	10.47	1.06	2.69	1.63	good
ls-li	13.14	12.94	4.12	3.65	0.47	great
NS-GN	63.98	62.19	5.43	8.17	2.74	good
MLr-MLl	45.07	45.03	1.92	1.85	0.07	great
CNr-CNl	36.13	35.63	2.27	2.42	0.15	great
chr-chl	44.00	43.89	3.40	2.32	1.08	great

Table 7 - values of linear distances, in mm, for operator (Op 1) and control operators (Op 2 and Op 3), for each subject, for evaluation of inter-observer variation.

Individual	PM-SD	ID-SM	ls-li	NS-GN	MLr-MLl	CNr-CNl	chr-chl
Op 1							
1118	12.74	5.46	11.79	68.14	45.76	37.17	37.22
1264	12.63	6.56	17.29	69.79	43.46	34.70	44.95
1265	8.57	5.38	10.31	62.52	42.09	38.69	42.14
1271	9.07	4.88	10.10	60.86	46.67	34.55	42.51
1272	9.14	5.61	13.10	53.27	48.20	37.26	47.72
1281	13.68	6.15	20.20	69.32	45.48	39.30	45.71
1283	8.92	5.85	7.63	64.14	43.94	34.15	44.34
1284	9.86	8.34	14.72	63.83	44.94	33.19	47.41
Op 2							
1118	12.12	5.62	11.40	68.31	45.63	37.47	41.42
1264	12.24	6.32	18.06	68.82	43.46	35.50	48.81
1265	7.57	6.92	11.60	62.75	42.56	35.63	45.75
1271	9.00	6.82	12.31	59.76	48.20	37.18	45.49
1272	9.14	5.24	13.24	53.34	48.49	38.60	52.76
1281	14.34	7.82	20.17	68.61	46.80	41.64	43.90
1283	9.04	7.00	9.61	62.77	43.17	35.40	56.02
1284	11.53	10.14	14.01	65.14	45.38	36.89	43.43
Op 3							
1118	10.39	5.80	9.62	68.87	44.84	36.92	39.47
1264	12.64	4.40	19.78	68.58	41.93	34.15	44.21
1265	7.90	4.60	9.53	62.98	40.90	38.77	45.62
1271	9.27	3.21	12.37	60.73	46.26	33.73	38.55
1272	7.58	2.87	14.12	54.06	47.82	37.15	46.35
1281	12.56	7.84	22.18	69.02	45.08	39.57	44.80
1283	6.57	6.12	7.26	64.14	43.44	35.34	45.73
1284	8.97	1.59	13.19	64.08	44.06	33.34	43.98

Table 8 – Averages of linear distances in mm, for inter-observer variation of operator 1 (Op 1) and control operators (Op 2 and Op 3). Difference between (DSD) largest and smallest standard deviation (SD 1, SD2 and SD 3) values were used to evaluate measurement reproducibility, considered good when 1.5 mm<DSD<3.0 mm or great when 0 mm<DSD<1.5 mm.

Measure	Op 1	Op 2	Op 3	DP 1	DP 2	DP 3	DSD	Reproducibility
PM-SD	10.58	10.62	9.49	2.08	2.27	2.24	0.20	great
ID-SM	6.03	6.99	4.55	1.06	1.51	2.01	0.95	great
ls-li	13.14	13.80	13.51	4.12	3.57	5.16	1.58	good
NS-GN	63.98	63.69	64.06	5.43	5.32	5.08	0.35	great
MLr-MLl	45.07	45.46	44.29	1.92	2.27	2.24	0.35	great
CNr-CNl	36.13	37.29	36.12	2.27	2.08	2.35	0.26	great
chr-chl	44.00	47.20	43.59	3.40	5.00	2.94	2.05	good

For SM and GN landmarks (table 4), the difference detected can be also explained by the variations of their distances from the mid-sagittal line, sometimes more slightly to its left or right (x axis, lateral-lateral direction). However, as the landmark stands on a concavity, the slight differences for the z axis (table 3) suggest that this craniometric point was also properly located on the cranial-caudal direction.

For the CNr landmark on inter-observer variation (table 4), the largest dmax detected, it is observed (table 3) that the largest differences between the axis are on the dorsal-ventral (y) axis. This suggests that variations occurred on the placement the landmark on the canine tooth, sometimes on its buccal surface (more anterior) and sometimes on its proximal surface (more posterior). This is a difficult landmark to locate, because observers may perceive the cranio-caudal level of the proximal surface differently. Still, a maximum difference of 3 mm should not interfere on measurements severely, if one considers that this is an extreme value, and the average distance stands around values lower than 2 mm. The same is worth for all of the landmarks that showed the largest values of dmax. Therefore, this interference on the process of landmark location can be a reflection of the statistically insignificant differences detected among the coordinates, for each axis.

With proper locations of both hard soft tissue landmarks, an adequate starting point for the linear measurements was established. Therefore, both intra- and inter-observer linear measurements and showed adequate reproducibility, with most of the discrepancies explainable by the ability of the operator to draw a line between circles. Despite the presence of 1.5 mm of diameter green circles, which work as a reference for landmark delimitation, there is no guarantee that the lines drawn by the operators were placed

exactly in their centers, although this would be desirable. Furthermore, a personal computer is not an instrument of great precision when a person must draw straight lines on its screen, so it can be inferred that the use of DICOM viewers that operate this way will always present a level of inaccuracy related to manual operation. Nonetheless, the differences between the standard deviations indicate good reproducibility.

CONCLUSION

Intra-observer and inter-observer variations did not hamper the use of the software as a tool for anthropometric studies. The use of OsiriX is an alternative in the anthropological study of craniofacial hard and soft tissues from CBCT scans.

ACKNOWLEDGEMENTS

The corresponding author would like to thank CAPES Foundation for granting scholarship for PhD studies, under Process 11215-12-7.

REFERENCES

1. Tedeschi-Oliveira SV, Melani RF, de Almeida NH, de Paiva LA. Facial soft tissue thickness of Brazilian adults. Forensic Sci Int 2009;193(1-3):127 e1-7.

2. Verze L. History of facial reconstruction. Acta Biomed 2009;80(1):5-12.

3. Farkas LG. Anthropometry of the head and face. Detroit, Michigan. Raven Press; 1994.

4. Ferrario VF, Sforza C, Poggio CE, Schmitz JH. Facial volume changes during normal human growth and development. Anat Rec 1998;250:480-7.

5. Sforza C, Grandi G, Binelli M, Tommasi DG, Rosati R, Ferrario VF. Age- and sex-related changes in the normal human ear. Forensic Sci Int 2009;187(1-3): 110e1-7.

6. Sforza C, Grandi G, Catti F, Tommasi DG, Ugolini A, Ferrario VF. Age- and sex-related changes in the soft tissues of the orbital region. Forensic Sci Int 2009; 185(1-3):115e1-8.

7. Sforza C, Ferrario VF. Three-dimensional analysis of facial morphology: growth. development and aging of the orolabial region. Ital J Anat Embryol 2010;115(1-2): 141-5.

8. Sforza C, Grandi G, De Menezes M, Tartaglia GM, Ferrario VF. Age- and sex-related changes in the normal human external nose. Forensic Sci Int 2011;204(1-3): 205 e1-9.

9. Cavanagh D, Steyn M. Facial reconstruction: soft tissue thickness values for South African black females. Forensic Sci Int 2011;206(1-3):215 e1-7.

10. Santos WDF. Mensuração de tecidos moles da face de brasileiros vivos em imagens multiplanares de Ressonância Magnética Nuclear (RMN) para fins médico-legais [thesis]. Ribeirão Preto: Universidade de São Paulo; 2008.

11. Sahni D, Sanjeev, Singh G, Jit I, Singh P. Facial soft tissue thickness in northwest Indian adults. Forensic Sci Int 2008;176(2-3):137-46.

12. Codinha S. Facial soft tissue thicknesses for the Portuguese adult population. Forensic Sci Int 2009;184(1-3):80e1-7.

13. Utsuno H, Kageyama T, Deguchi T, Umemura Y, Yoshino M, Nakamura H, et al. Facial soft tissue thickness in skeletal type I Japanese children. Forensic Sci Int 2007;172(2-3):137-43.

14. Utsuno H, Kageyama T, Uchida K, Yoshino M, Oohigashi S, Miyazawa H, et al. Pilot study of facial soft tissue thickness differences among three skeletal classes in Japanese females. Forensic Sci Int 2009;195(1-3):165 e1-5.

15. El-Mehallawi IH, Soliman EM. Ultrasonic assessment of facial soft tissue thicknesses in adult Egyptians. Forensic Sci Int 2001;117(1-2):99-107.

16. De Greef S, Claes P, Vandermeulen D, Mollemans W, Suetens P, Willems G. Large-scale in-vivo Caucasian facial soft tissue thickness database for craniofacial reconstruction. Forensic Sci Int 2006;159 Suppl 1:S126-46.

17. Rhine JS, Campbell HR. Thickness of facial tissues in American blacks. J Forensic Sci 1980;25(4):847-58.

18. Smeets D, Claes P, Vandermeulen D, Clement JG. Objective 3D face recognition: Evolution. approaches and challenges. Forensic Sci Int 2010;201(1-3):125-32.

19. Rocha SS, Ramos DL, Cavalcanti MG. Applicability of 3D-CT facial reconstruction for forensic individual identification. Pesqui Odontol Bras 2003; 17(1):24-8.

20. Kim KD, Ruprecht A, Wang G, Lee JB, Dawson DV, Vannier MW. Accuracy of facial soft tissue thickness measurements in personal computer-based multiplanar reconstructed computed tomographic images. Forensic Sci Int 2005;155(1):28-34.

21. Fourie Z, Damstra J, Gerrits PO, Ren Y. Accuracy and reliability of facial soft tissue depth measurements using cone beam computer tomography. Forensic Sci Int 2010;199(1-3):9-14.

22. Fourie Z, Damstra J, Gerrits PO, Ren Y. Evaluation of anthropometric accuracy and reliability using different three-dimensional scanning systems. Forensic Sci Int 2010;207(1-3):127-34.

23. Pereira CB, de Mello e Alvim MC. Manual para estudos craniométricos e cranioscópicos. Santa Maria, Brazil; 1979.

24. University of Pittsburgh, National Institute of Dental and Craniofacial Research's FaceBase [Internet]. [updated 2013 Jul 30; cited 2013 Aug 20]. Available from: http://www.facebase.org/.

25. Gwilliam JR, Cunningham SJ, Hutton T. Reproducibility of soft tissue landmarks on three-dimensional facial scans. Eur J Orthod 2006;28(5): 408-15.